DOUBLE-SKIN SYSTEM OF ROOM-SIDE AIR GAP APPLIED TO DETACHED HOUSE (PART 2): SIMULATION ANALYSIS TO REDUCE COOLING LOAD THROUGH NATURAL VENTILATION IN WALL

Togo Yoshidomi[1], Shinsuke Kato[*2], Kan Lin[3], and Kyosuke Hiyama[4]

1 Graduate School of The University of Tokyo
7-3-1, Hongo, Bunkyo-ku,
Tokyo, Japan

2 IIS, The University of Tokyo
4-6-1 Komaba, Meguro-Ku,
Tokyo, Japan
**Corresponding author: kato@iis.u-tokyo.ac.jp*

3 Graduate School of The University of Tokyo
7-3-1, Hongo, Bunkyo-ku,
Tokyo, Japan

4 Yamaguchi University
1677-1, Yoshida, Yamaguchi-shi,
Yamaguchi, Japan

ABSTRACT

In Japan, wooden detached residential houses are common; the wood components within a wall may undergo decay because of condensation in the wall or flushing defects, which can be a concern. The temperature distribution throughout the house, such as a high temperature in the attic space, can cause discomfort to the occupants. A double-skin system of room-side air gaps is considered to be an effective technique to handle these problems. In this system, during the summer, the airflow driven by natural ventilation moves through the room-side air gap in the wall and removes heat load from the inner surface of the insulation material or from the surface adjacent to the rooms inside. Although this system has been applied to many houses, further study on the design specifications for parts of the ventilation route is still required. In this study, airflow network simulation was carried out using TRNFlow to evaluate the performance of this system under different conditions. A standard residential house model was simulated by considering conditions of summer. On the basis of the results, it was verified that the total airflow rate exhausted from the rooftop vent fluctuates with the ambient temperature; the flow rate distribution in different walls was also determined. Sensitivity analysis was performed on each part of the ventilation route with different opening areas; the opening area of the wall was found to have more effect than the rooftop and base vents on the total amount of airflow. When wind is blowing outside, the total flow rate increases. When there is no wind outside and the windows are closed, this system reduces the cooling load of an ordinary detached house by 15.5%.

KEYWORDS

Double-skin system, Detached house, Simulation, Natural ventilation, Cooling load

1 INTRODUCTION

In Japan, wooden detached houses, which have a wooden structure and insulation material, are popular. However, several problems are associated with this type of house. In the summer, a temperature distribution can be caused by heat from solar radiation. In the winter period, if the house is not sufficiently airtight, moist air leaking from the room is cooled by the outside air, and condensation occurs in the wall. This condensation may cause the wooden structure to decay. To remove moisture in the wall, vent layers are now often installed outside the insulation material to exhaust the moisture, and Hokoi (Hokoi, 2011) has done measurements and calculations.

The double-skin system of a room-side air gap, which places the vent layer inside the insulation material, has also been applied to detached houses. The air gap extends to envelope the entire house, and ventilated air can move freely in the gap. The airflow pattern in the air gap differs in the summer and winter. In the summer, air vents at the top of the roof and sides of the base are opened to introduce and discharge outside air. When the air in the air gap is heated by solar radiation and rooms inside the wall, an upward driving force is generated because of buoyancy. Thus, a flow is induced where outside air is introduced through vents at the base; it moves upward through the wall and flows out through the roof. This airflow discharges heat in the wall and attic space while being cooled by the ground under the floor, so the rooms are kept at a comfortably moderate temperature and. In the winter, all of the vents are closed to increase thermal insulation and air circulation in the air gap.

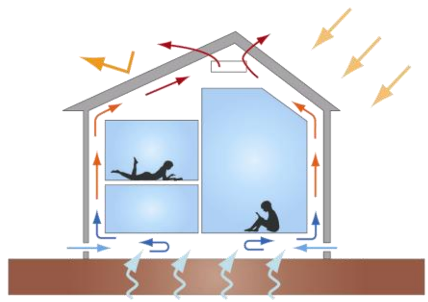
Figure 1: Double-skin system of room-side air gap applied to detached house

Although some houses in Japan have been built using this system for about 30 years, few studies have examined the system in detail. Ozaki et al. measured temperature and humidity in the air gap in wall of an experimental house during the summer rainy season.

However, there have been no studies on how to obtain sufficient airflow and the effects of introducing this system. With respect to the airflow rate, quantifying the effects of the air gap specifications and outside disturbances is necessary. With regard to the air gap specifications, both the opening areas with the smallest cross-sections in the air gap and the leakage area of the entire house are considered. Since the smallest cross-sections in the air gap can play a major role in determining the overall ventilation resistance of the entire air gap, the airflow rate may get affected if different opening areas are used for these parts. If the leakage area is increased, infiltration of the air gap, rooms, and outside air will increase, and the airflow rate of the original route will decrease. With regard to outside disturbances, external wind was considered. The effect of external wind seems to depend on the relationship between the vent position and the wind pressure coefficient distribution of the outer wall surface along with the wind speed and direction. With respect to the effect of introducing the system, quantifying the effect on the thermal environment is necessary. This can be confirmed by verifying that the natural room temperature and air-conditioning load decrease during the summer period when this system is introduced. When air-conditioning is on, some of the cooling air supplied by the air-conditioner will be ejected outside by the airflow, so the air-conditioning load might actually increase. Therefore, examining the effect on the load reduction due to the shortened air-conditioning time is also necessary.

This study aimed to determine the basic properties of the double-skin system of a room-side gap during the summer through the simulation of a ventilation network. We created two building models in which spaces in the air gap and rooms of the house were treated as individual nodes. The impact of each element on the airflow rate was estimated, and the effect of introducing this system was simulated. For the airflow rate, a sensitivity analysis was performed on the opening area of each airflow resistance part by using a building model without infiltration. The results show the relationship between the airflow rate and different opening area patterns. For the external wind, the impact on the airflow rate was examined under several conditions. The effect of infiltration on the airflow rate was estimated by comparing a model of a general detached house with infiltration to the model with no infiltration. For the introduction effect, the natural room temperature for the middle of summer was calculated using the model with infiltration, and the decrease in the natural room temperature was estimated when the system was used. We calculated the air-conditioning load using the same model and compared it to the result for the case when there was no airflow in the wall. Preventing condensation inside the wall by considering the humidifying capacity of the wall is outside the scope of this study.

2 METHODS

2.1 Simulation Software

To calculate the airflow in the air gap, we used the unsteady energy calculation software TRNSYS17 and its add-on program TRNFlow. TRNFlow is based on COMIS3.1, which is a ventilation network calculation software that can iteratively solve the movement of air and heat simultaneously on TRNSYS. We used this software to solve the airflow in the air gap.

2.2 Building Models

We used the standard house model (fourth region) proposed by IBEC, Institute for Building Environment and Energy Conservation, to represent a standard detached house in Japan. This model has two stories and a total floor area of 120.07 m^2. A family of four people is supposed to live in there. Schedules for the occupants, lighting, equipment, ventilation, and air-conditioning were based on the survey results. We set up the dimensions and basic configuration of the building according to this model.

We modeled the air gap, which may significantly affect the calculation of airflow in the wall, as follows. In figure 3, the area of the air gap where air moves around is represented in blue. Grooves are placed at equal intervals on the surface of the insulation used in the walls; these grooves ensure that openings between the insulation and other components do not impede airflow. The air gap can be divided into several zones by the resistance parts such as vents or these openings, where the flow path is narrower than other parts. For the TRNFlow calculations, we modeled the air gap by defining this zone as “air node” and defining the resistance part as “air link.” For each air link, the relationship between the mass flow rate and pressure difference was calculated according to equation (1). In equation (2), which is the common formula for ventilation, the value of C_s for each air link was determined by fixing α to 0.6, which is a typical value, and determining the opening area A of the air link from the actual specifications of the house. The value of n was determined to be 0.5 from the correspondence between formula (1) and equation (2).

$$\dot{m} = C_s \cdot (\Delta p)^n \tag{1}$$

$$\dot{m} = \alpha A \sqrt{2\rho \cdot \Delta p} \tag{2}$$

$\dot{m}$: Δp mass flow rate [kg / h], α: pressure difference [Pa], C_s: flow coefficient [-],
A: opening area [m2], ρ: air density [kg/m^3]

In this study, two building models with different air link networks were created: a “simple model” that does not consider infiltration and a “detailed model” that does. In the simple model, the leakage of air into the rooms or outside air from the air gap is not considered; a simple network that connects the air gap to the outside air was created, as shown in figure 4 and 5. This model can be used to estimate the potential maximum airflow generated by buoyancy ventilation without depending on the amount of infiltration. However, because heat from solar radiation and internal heat cannot be discharged by infiltration, the calculated room temperature may be higher than the actual environment. On the other hand, the detailed model considers infiltration between air nodes; the network is shown in figure 6. The typical C-value of this house was assumed to be 2 cm^2/m^2; values for surfaces were allocated to the walls, openings such as windows and doors, and the ventilation equipment. The allocation percentage was determined by referring to the measured data of a general detached house. This model is suitable for calculating the room temperature and air-conditioning load because its approach considers the actual environment. However, the results calculated with this model depend on the size and distribution of the opening areas.

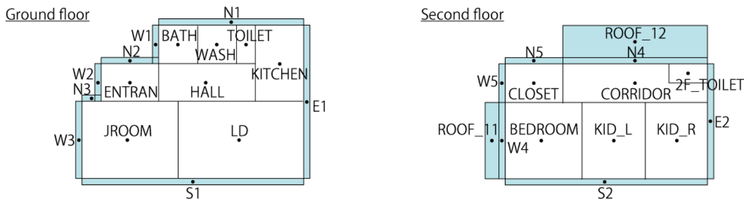

Figure 2: Zones and air nodes of the building model in TRNSYS

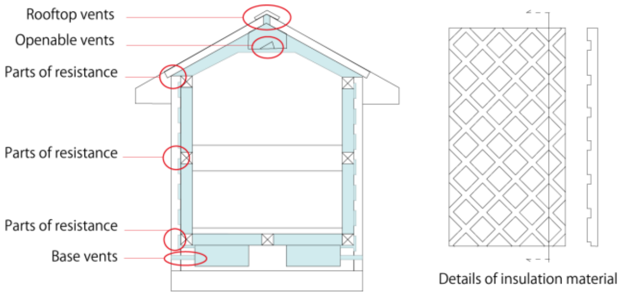

Figure 3: Overview of air gap and insulation material

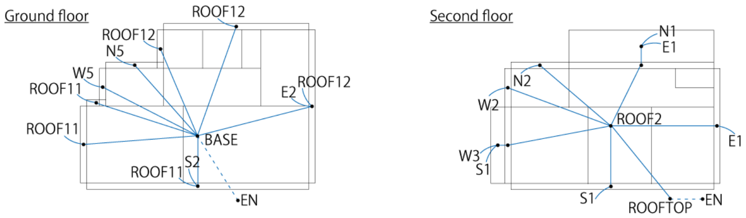

Figure 4: All air links set in TRNFlow (simple model)

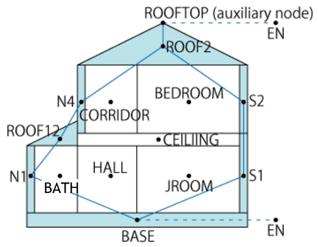

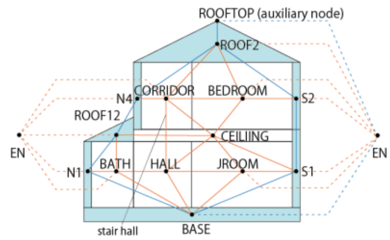

Figure 5: Overview of air links (simple model)

Figure 6: Overview of air links (detailed model)

Table 1: Calculation conditions for building

Wall of external side	Extruded polystyrene foam 50 mm + Air layer 15 mm + Tile 10 mm
Wall of internal side	Gypsum board 13 mm
Air gap thickness	120 mm
Roof	Extruded polystyrene foam 50 mm + Air layer 30 mm + Plywood 10 mm + Slate 5 mm
Base	EPS 50 mm + RC150 mm + EPS 50 mm
Internal wall, Ceiling, Floor	U = 3.125 W/m^{2}K, 4.082 W/m^{2}K, 4.082 W/m^{2}K
Window	Double-glazing U = 1.8 W/m^{2}K, Shading coefficient = 0.5
Infiltration	None

Table 2: Calculation conditions for air gap

Opening area A [m^2]	Openings in the wall	0.00299 m^2/m (opening area per unit length wall)
	Roof vents (Vents at the rooftop)	0.0919
	Roof vents (Mechanical opening/closing unit in the attic space)	0.0755
	Base vents	0.0720
Constants		$\alpha = 0.6$, $\rho = 1.2$, $n = 0.5$

Table 3: Opening areas of infiltration (detailed model)

Opening areas of whole house1	Total floor area	120.07 m^2	
	C-value	2 cm^2/m^2	
	Opening area of whole house	240 cm^2	
Allocation of opening areas	Structure	94 cm^2	39%
	Opening	67 cm^2	28%
	Ventilating facilities	79 cm^2	33%
	(contains local ventilation)	64 cm^2	27 %
	(contains overall ventilation)	15 cm^2	6 %

2.3 Calculation Conditions

The calculation conditions are listed in Tables 4–8. To examine the airflow rate, two sensitivity analyses were carried out on the airflow rate for different opening areas of resistance parts and different external wind conditions. To examine the properties of the airflow rate, the simple model was used in these analyses. Table 4 lists the cases for the opening area. Eleven cases were calculated; the values of the opening areas for three elements—walls, rooftop vents, and base vents—were multiplied by 5 or 0.5. To examine the external wind, wind pressure coefficients C_p around the rooftop and base vents were set according to the specifications listed in Table 5. Each C_p value was determined using the average value, obtained from literature, for the wind pressure coefficient distribution of the building surface at the portion corresponding to each vent. Because the wind pressure coefficient varies according to objects around the building, we also used wind pressure coefficients under the conditions of surrounding buildings being present or absent. Table 6 lists the cases for the external wind. When there are surrounding buildings, wind pressure

Table 4: Cases for sensitivity analysis of opening area in air gap

	Resistance in air gap	**Rooftop vents**	**Base vents**
Case 1	-	-	-
Case 2	×5	-	-
Case 3	-	×5	-
Case 4	-	-	×5
Case 5	×0.5	-	-
Case 6	-	×0.5	-
Case 7	-	-	×0.5
Case 8	-	×5	×5
Case 9	-	×0.5	×0.5
Case 10	×5	×5	×5
Case 11	×0.5	×0.5	×0.5

Table 5: Calculation conditions of wind pressure coefficients

	Vents		**Wind direction**			
	Location	**Direction**	**North**	**East**	**South**	**West**
Case 12 (with surrounding building)	Rooftop vents	North	0	0	-0.18	0
		South	-0.18	0	0	0
	Base vents	North	0	0.01	0.05	0
		East	0.05	0.1	0.05	0.03
		South	0.05	0	0	0.01
		West	0.05	0.03	0.05	0.1
Case 13 (without surrounding building)	Rooftop vents	North	-0.2	-0.25	-0.55	-0.25
		South	-0.55	-0.25	-0.2	-0.25
	Base vents	North	-0.7	-0.3	0.22	-0.3
		East	-0.4	0.6	-0.4	-0.15
		South	0.22	-0.3	0.7	-0.3
		West	-0.4	-0.15	-0.4	0.6

Table 6: Cases for sensitivity analysis of external wind

	External wind	**Surrounding building**
Case 1	None	N/A
Case 12	Exist	Exist
Case 13	Exist	None

Table 7: Cases for introduction effect

	Airflow	**Air-conditioning**
Case 21	Exist	None
Case 22	Exist	Exist
Case 23	None	None
Case 24	None	Exist

Table 8: Calculation conditions

Internal heat gain	Exist (based on schedule by IBEC)
Ventilation	None, Exist (based on schedule by IBEC)
Air-conditioning	None, Exist (based on schedule by IBEC)
Surface temperature under floor space	20°C
Weather data	Expanded AMeDAS standard data (2000) Tokyo
External wind	None, Exist (based on weather data)
Calculation period	Jul. 21–Aug. 20, Jun. 1–Sep. 30 (plus 3 days for run-up period)

coefficient is generally smaller, and the impact of wind is reduced. In case 12, surrounding buildings were considered; buildings of the same shape were assumed to be arranged according to a density with a gross building coverage ratio of 40%, which is equivalent to the most overcrowded residential area in Tokyo.

To examine the effect of introducing the system, the detailed model was used to obtain a room temperature close to that of the actual environment. Table 7 lists the cases for the introduction effect. First, the airflow rate and natural room temperature were calculated without air-conditioning. Airflow rates calculated on the basis of the simple and detailed models were compared to examine the effect of infiltration. The results for the cases with and without airflow in the wall were then compared, and the effect of lowering the natural room temperature by means of airflow in the wall was examined. The calculation for the case without airflow was performed by removing all air links from the detailed model. Finally, to calculate the air-conditioned state, the effect of reducing the air-conditioning load due to airflow in the wall was estimated. The temperature was set to 28°C, and five rooms (i.e., living room, kitchen, bedroom, and two children's rooms) were air-conditioned. This time opening of windows when ambient temperature is lower than room temperature is not considered.

The other calculation conditions that were used are listed in Table 8. The schedules for internal heat generation, ventilation, and air-conditioning were set according to the criteria of the IBEC standard. Ventilation was used only in the detailed model. The ground surface temperature under the floor space was set to 20°C on the basis of past measurement results. For weather data, including for external wind, the expanded AMeDAS 2000 standard data for Tokyo was used. The calculation periods were July 21–August 20 (plus 3 days for the run-up period) to study the airflow rate and June 1–September 30 (plus 3 d for the run-up period) to study the introduction effect.

3 RESULTS

3.1 Airflow Rate

First, the results of the representative case 1 are shown to demonstrate the basic properties of the airflow rate: airflow rate of S1, the south side wall on the ground floor, and rooftop vents (figure 2), room temperature of LD, a living-dining room on the south side (figure 5), and outside temperature during representative days (August 8– 10; figure 7). The airflow rate in the rising direction within the network is represented as a positive value. The average airflow rate during the period was 114.8 m^3/h. The room temperature changed almost simultaneously with the outside air temperature, and peak hours were the same. On the other hand, the changes in airflow rate of the rooftop vents occurred 2–3 h later than the changes in the temperature. The airflow rate of S1, which can be taken as representative of each wall, changed almost proportionally to the flow rate of the rooftop vents. We discuss the time delay in section 4. Figure 8 shows the average flow rate per unit length of wall over the period for each wall. The light-colored bar represents the ground floor, whereas the dark-colored bar represents the second floor. The airflow rate was positive throughout the wall. The average airflow rate on the ground floor was 3.14 $(m^3/h)/m$, and the average on the second floor was 3.80 $(m^3/h)/m$.

Figure 9 shows the sensitivity analysis results for the opening areas. The bar graphs represent the airflow rates of the rooftop vents. The airflow rates of case 1 and the cases where the opening areas changed by 5× and 0.5× are shown together. In cases 2–7, only one element was changed; the results were highly sensitive to changes in the wall, rooftop vents, and base vents, in descending order. The changes in airflow rate were smaller than the ratio of the changes in the opening areas. In cases 8–11, multiple elements were changed. The change in airflow rate was significantly greater when all three elements were changed (case 10); the change in airflow rate was close to the change in opening area ratio (0.54×) in case 11.

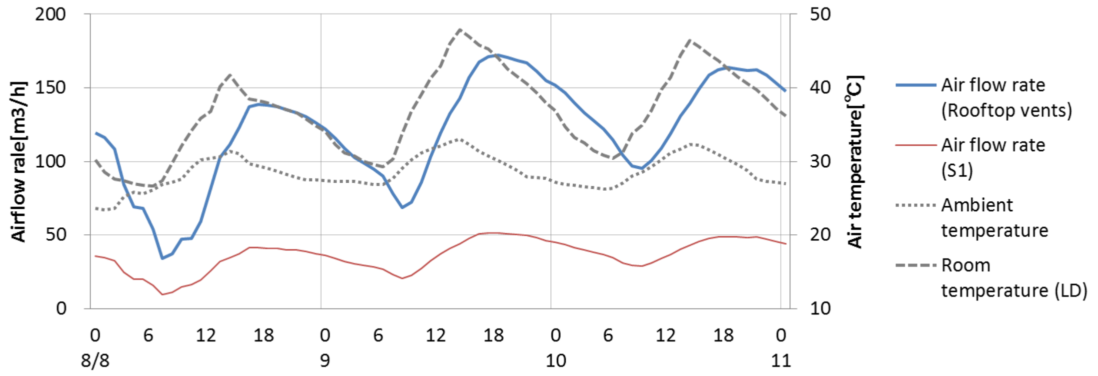

Figure 7: Airflow rate and ambient and room temperatures on representative days

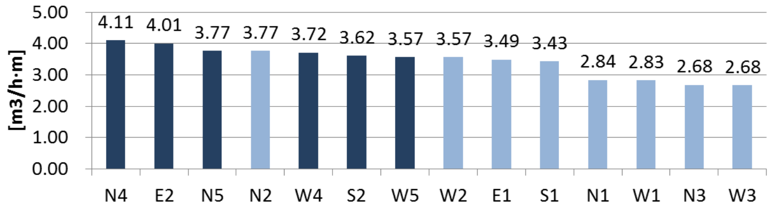

Figure 8: Airflow rate per unit length wall of each wall

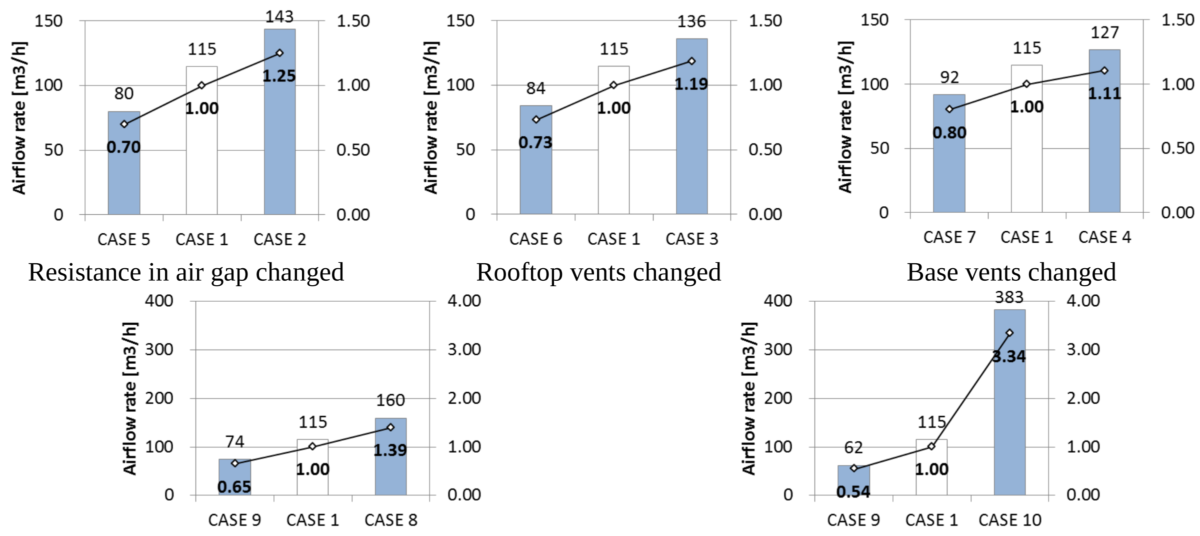

Figure 9: Average airflow rate over period

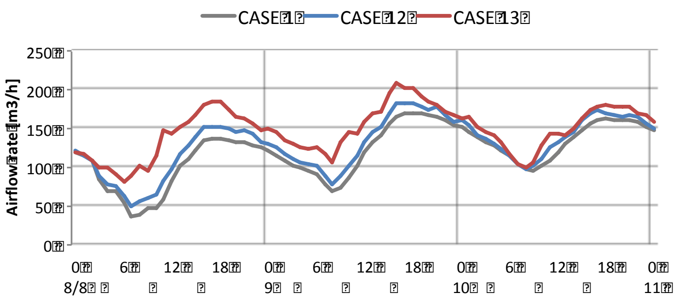

Figure 20: Airflow rate in the representative days

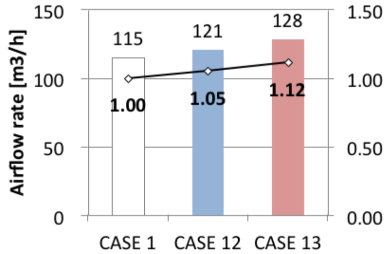

Figure 31: Period average airflow rate

Figures 10 and 11 show the sensitivity analysis results for external wind. The line and bar graphs indicate the airflow rate of the rooftop vents. Figure 10 shows the change in airflow over time during the representative days; the airflow rate fluctuated proportionally in all cases. Figure 11 shows the average airflow over the period in each case. Compared with the case of

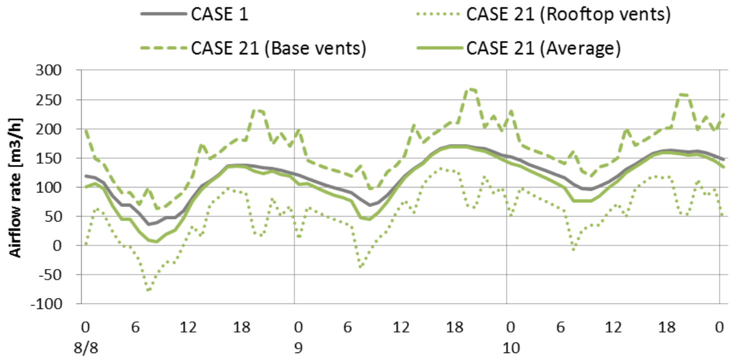

Figure 12: Airflow rate during representative days

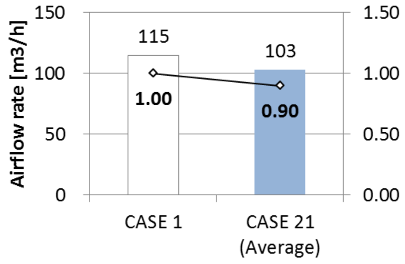

Figure 43: Average airflow rate over period

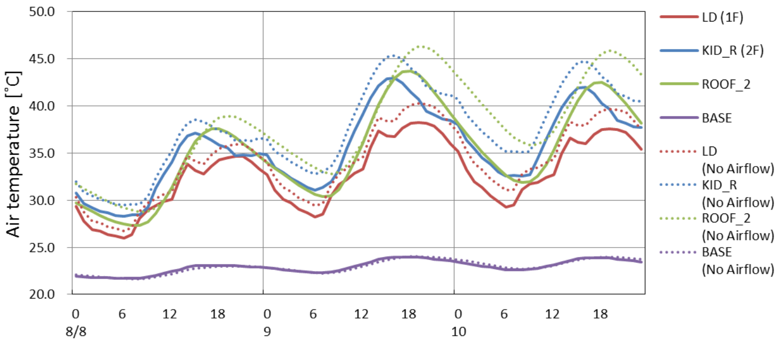

Figure 54: Natural room temperature during representative days

Table 9: Differences in average natural temperature over period by airflow in air gap

Zone	Average temperature difference
Average of 1F	-1.53
Average of 2F	-1.87
Rooftop vents (1F and 2F)	-2.43
Under floor space	1.03

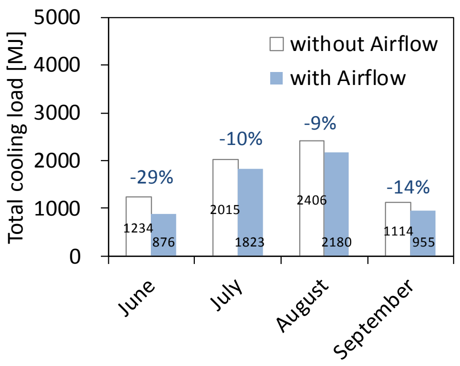

Figure 16: Total cooling load in each month

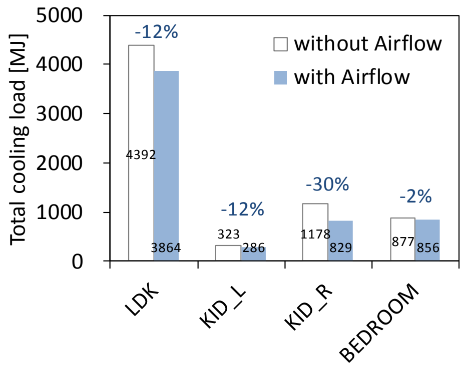

Figure 17: Average cooling load in each room over period

no wind, the average airflow increased by 5% for the case with surrounding buildings and increased a further 5% for the case with no surrounding buildings.

3.2 Introduction Effect

The detailed model that considers infiltration was used to examine the introduction effect. Figure 12 compares the airflow rates of the detailed model (case 21) and simple model (case 1) over time. In case 1, the airflow rates of the base vents and rooftop vents were equal; they are represented by a gray line. In case 21, the airflow rates of the base vents and rooftop vents were different; they are represented by dotted lines. The average airflow rates of the base vents and rooftop vents can be assumed to represent the airflow characteristics throughout the building in case 21; the change in this value over time showed properties similar to those of case 1. Figure 13 shows the average airflow over the period of both cases. For case 21, this average value was used. In case 21, when infiltration was considered, the airflow rate decreased by 10%.

The details for the natural room temperature during the representative days are given in Table 9 and Figure 14. Solid lines represent the natural room temperature for the case when there is airflow (case 21), and the dotted lines represent the natural room temperature for the case without airflow (case 23). The temperature was higher on the second floor than on the first floor. The average natural room temperature on the first floor decreased 1.5 °C with airflow, and that of the second floor decreased 1.9 °C. While the average temperature of the attic spaces for the first and second floors decreased 2.4 °C, the average under the floor space rose 1.0 °C.

Figure 16 shows the total cooling load for each month when the air-conditioning was set at 28°C. The monthly total cooling load of the whole house with airflow (case 22) and without airflow (case 24) is represented in the graph. The cooling load was reduced when there was airflow throughout the month; from June to September, it was reduced by an average of 15.5%. The reduction was large in June and September, which had low temperatures; even in August, which was the hottest month, saw the cooling load reduced by 9%. Figure 17 also shows the total cooling load for each room from June to September. The amount of reduction varied in each room; it was 2%–30%.

4 DISCUSSION

4.1 Airflow rate

Figures 7 and 8 show that the airflow rate in the representative case was uniform in each wall, and the variation in airflow over time in each wall was approximately proportional to the airflow rate of the rooftop vents. Therefore, the variation in airflow of the whole building can be represented by the airflow rate of the rooftop vents; the airflow rates were thus compared by using the airflow rates of the rooftop vents.

The flow rate of the rooftop vents changed 2-3 hours after the outside air temperature. This is considered to be due to effects that heat stored in the wall is discharged by the airflow. In other words, heat from hot outside air and solar radiation stored in the components on the outside of the air gap leads to air temperature rise in the air gap and an increase in the pressure difference between the inside and outside, and contributes to the delay of the airflow. On the other hand, it is considered that because the influence of the heat storage to the room is reduced by the airflow, room temperature changed in the same phase as the outside air temperature. Therefore, possibility of controlling the flow of heat stored in the wall into the rooms by controlling the airflow is suggested. For example, the cold heat is stored in the wall by the airflow at night, also in the morning the airflow is stopped to take the stored cold heat into the rooms, and in the afternoon the airflow is resumed to keep the stored heat by the sunlight from flowing in the room. By performing these operations, improving of the energy saving effect by the airflow can be expected.

In the sensitivity analysis of the vent opening area, the magnitude of the sensitivity of the opening areas of each portion in the air gap became clear. Although the magnitude of the sensitivity varied in cases, especially when the opening areas of all elements were changed in the same manner, the airflow rate changed significantly. The airflow rate increased 1.39 times when two elements were changed in case 8; the airflow rate increased 3.34 times when three elements were changed in case 10. When the opening area was changed to 0.5×, the airflow rate was significantly reduced by only changing one or two elements (cases 5–7, 9, and 11). This result seems to show that the flow rate of the whole air gap depends on the magnitude of the resistance at points where the airflow resistance is high. The airflow increased when there was an external wind, and the airflow became particularly large when there were no surrounding buildings. This is because the wind pressure coefficient, listed in Table 5, was lower at the rooftop vents than that at the base vents, and more work was required to draw the air out of the air gap. Since this pressure difference was higher for the case without surrounding building than for the case with them, the increase in airflow rate became larger.

4.2 Introduction Effect

The magnitude of the effect of infiltration on the airflow rate was estimated by comparing the results of the simple and detailed models (Figure 13). When the C-value was 2 cm^2/m^2 and the opening area was assumed to be allocated as listed in Table 3, the airflow rate was reduced by 10% with infiltration. The natural room temperature was lowered whenever there was airflow. While the temperature under the floor space was increased by the outside airflow, the temperature in the attic space dropped as more hot air was discharged. The introduction effect was expected to be dependent on the cooling supplied from the ground surface under the floor to the air gap. Although the ground surface temperature was set to 20°C on the basis of past measurement results, a detailed simulation of geothermal heat is necessary for future study.

When air-conditioning was used, the total period of the air-conditioning load was reduced. We should note that there was no opening of windows in this calculation. Figure 18 shows the total time that air-conditioning was active for each month. This value was reduced when there was airflow, and this trend was close to the result of cooling load (Figure 16). Therefore, the reduction in the cooling load period is mainly due to the reduction in air-conditioning time.

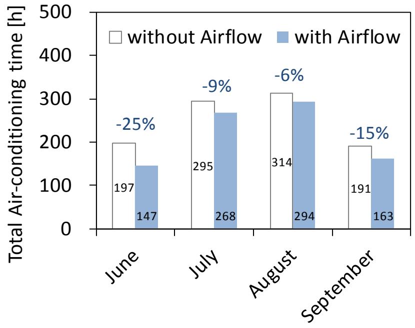

Figure 18: Total air-conditioning time in each month

5 CONCLUSIONS

We simulated a ventilation network to examine the airflow rate in the air gap and the introduction effect. In the simple model, infiltration was not considered, and it was found that the air rose uniformly in any wall surface; it was discharged from roof vents. The airflow rate changed 2–3 h after the outside air temperature. Sensitivity analysis of the opening areas in the air gap for the airflow rate showed high sensitivity to changes in the wall, rooftop vents, and base vents, in descending order. The airflow rate changed significantly when the opening areas of all three elements were changed similarly. Sensitivity analysis of the external wind effect on the airflow rate showed that the airflow rate increased in the case with an external wind compared to the case without an external wind. In particular, the case of no surrounding buildings caused the pressure difference between the inlet and outlet of the vents to increase, and the airflow rate increased significantly.

We examined the effect of introducing the double-skin system of room-side air gap by using a detailed model that considers infiltration. When this system was introduced, the natural room temperature was lowered throughout the summer compared to the case without ventilation. However, since the room temperature still exceeded the comfort zone in the summer, air-conditioning was required. The total cooling load of the period was reduced when there was airflow in the wall with air-conditioning. This effect is mainly due to the reduction in air-conditioning time caused by the drop in room temperature. The introduction effect was assumed to depend on the cooling supplied from the ground surface under the floor to the air gap, so a detailed simulation of geothermal heat is necessary for future study.

6 REFERENCES

Hokoi, S. (2011). Survey of Ventilation Volume in the Vented Air Space of Exterior Walls [in Japanese]. *Summaries of technical papers of Annual Meeting Architectural Institute of Japan, D-2,* 839-840.

Ozaki, A. (1992). Heat and water transfer through an ventilated structure using urethane panels [in Japanese]. *Summaries of technical papers of Annual Meeting Architectural Institute of Japan, D,* 945-946.

Institute for Building Environment and Energy Conservation. (2009). *Description of the energy consumption calculation method in the standards of judgment of the housing business building owners* [in Japanese]. http://ees.ibec.or.jp/documents/img/kaisetsu200903_all_ver2.pdf

Kurabuchi, T. (2009). Wind tunnel experiments on surface wind pressure and cross-ventilation flow rate in densely populated residential area: study on proper design method of locating windows aiming at utilization of cross-ventilation in densely populated residential area (part 1) [in Japanese]. *Journal of environmental engineering 74(642), 951-956*.